

Suppression of near-surface scattered body to surface waves: steerable and non-linear filter approach

Abdulaziz M. Almuheidib* and M. Nafi Toksöz, Earth Resources Laboratory, MIT

SUMMARY

We present an approach based on local-slope estimation for the separation of scattered surface waves. The near-surface scattered body-to-surface waves, which have comparable amplitudes to reflections, can mask the seismic reflections. These difficulties, added to large amplitude direct and back-scattered surface (Rayleigh) waves, create a major reduction in signal-to-noise ratio and degrade the final subsurface image quality. Removal of these waves can be difficult using conventional filtering methods, such as an $f - k$ filter, without distorting the reflected signal. The filtering algorithm we present is based on predicting the spatially varying slope of the noise, using steerable filters, and separating the signal and noise components by applying a directional non-linear filter oriented toward the noise direction. The slope estimation step using steerable filters is very efficient. It requires only a linear combination of a set of basis filters at fixed orientation to synthesize an image filtered at an arbitrary orientation. We apply our filtering approach to simulated seismic data and demonstrate its superiority over conventional $f - k$ techniques in signal preservation and noise suppression.

INTRODUCTION

In land seismic data, the direct and scattered surface waves contain a significant amount of seismic energy and present great challenges in data acquisition and processing, especially in arid regions with complex near-surface heterogeneities (e.g., dry river beds, wadis/large escarpments, and Karst features). A significant fraction of the seismic energy is trapped and scattered in the near-surface layers (in the form of coherent noise) and masks the body wave reflections from deeper structures. In case of a surface seismic source, the main components of surface related noise include: (1) direct surface waves; (2) forward and back-scattered surface waves; and (3) body-to-surface scattered waves (Figure 1). The upcoming body wave reflections (e.g., P and S waves including primaries, multiples and mode conversions) impinge on the near-surface heterogeneities and scatter to weak P and S waves, and also to Rayleigh waves since the heterogeneities act as secondary elastic sources. In a previous study (AlMuheidib and Toksöz, 2014), we demonstrated the scattering from near-surface heterogeneities using the perturbation theory and finite difference modeling, and showed that the scattered field is equivalent to the radiation field of an equivalent elastic source excited at the scatterer locations. In conventional seismic data processing, these scattered body-to-surface waves are not usually removed.

Surface waves, in general, are characterized by low frequency, linear moveout, large amplitudes and slow amplitude decay with distance. The direct surface wave is confined within a fan-shaped window in the time-space domain and is much larger in amplitude and lower in frequency than body wave reflections.

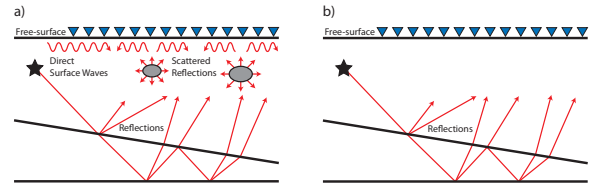


Figure 1: Schematic earth model showing: (a) scattering of direct surface and reflected body-waves to surface waves, and (b) the ideal model after removing the effects of scattering.

These characteristics of direct surface waves make it effective to apply filtering techniques within this narrow fan-shaped window. However, the scattered body-to-surface waves have comparable amplitudes to reflections, frequencies dependent on the size of the scatterers, and they mask the entire dataset. These challenges make it difficult to reduce these noise features using conventional filtering methods, such as an $f - k$ filter.

NOISE REDUCTION BY SPATIAL SLOPE ESTIMATION

To overcome the drawbacks of most conventional filtering methods, we propose a new filtering algorithm that exploits the multidimensionality of the seismic data to obtain more reliable results of signal and noise separation. The approach suppresses locally-linear scattered surface waves by first estimating the dominant local-slopes as a function of offset using steerable filters (Freeman and Adelson, 1991), and then applies a local non-linear median filter oriented toward the noise direction, assuming the moveout of the noise is locally linear. The estimated dominant local-slopes may vary as a function of offset (or patch of receivers), which makes this approach applicable in case of lateral velocity variations or surface topography.

Steerable filters

Oriented filters are used in many vision and image processing tasks such as edge detection, texture analysis, segmentation, motion analysis, and image enhancement and compression. The steerable filter is one of a class of filters in which a linear combination of a set of basis filters at fixed orientation is used to synthesize a filter of an arbitrary orientation (Freeman and Adelson, 1991; Simoncelli and Freeman, 1995). It is useful to examine filter outputs (images) as a function of phase and orientation, efficiently, without the need to apply many versions of the same filter rotated at different angles. The idea of the steerable filter can be simply illustrated using the partial derivative of a 2D symmetric Gaussian filter

$$G(x, y) = e^{-(x^2 + y^2)}. \quad (1)$$

The first x and y derivatives of a Gaussian are

$$G^{0^\circ} = -2xe^{-(x^2 + y^2)}, \quad (2)$$

Suppression of near-surface scattered body to surface waves

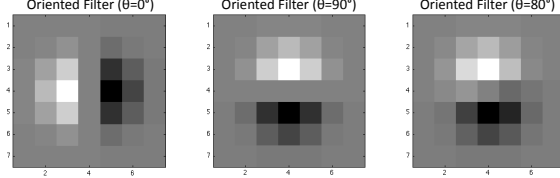


Figure 2: Derivatives of Gaussian filters: (left) basis filter oriented at 0° , (middle) oriented at 90° , and (right) synthesis of the filter oriented at 80° by linearly combining the basis filters.

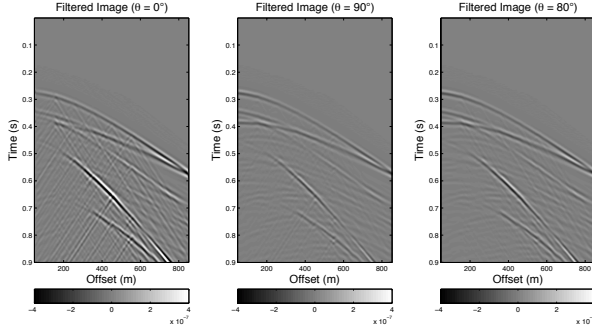


Figure 3: Convolution of the input image with different directional filters: (left) with a basis filter oriented at 0° , (middle) with a basis filter oriented at 90° , and (right) synthesis of the image filtered at 80° orientation by linearly combining the convolution of the input image with the basis filters.

$$G^{90^\circ} = -2ye^{-(x^2+y^2)}. \quad (3)$$

Therefore, we can synthesize a filter at an arbitrary orientation θ as shown in Figure 2 by taking a linear combination of x and y derivatives (basis filters):

$$G^\theta = \cos(\theta)G^{0^\circ} + \sin(\theta)G^{90^\circ}. \quad (4)$$

We can synthesize a seismic image filtered at an arbitrary orientation $R(x, y, \theta)$ as shown in Figure 3 by convolving the input image $I(x, y)$ with the directional filter G^θ

$$R(x, y, \theta) = \cos(\theta)(G^{0^\circ} * I(x, y)) + \sin(\theta)(G^{90^\circ} * I(x, y)). \quad (5)$$

Slope estimation of local plane-waves

The local plane-wave PDE (Fomel, 2002) is given as

$$\left(\frac{\partial}{\partial x} + s(\mathbf{x}, \mathbf{t}) \frac{\partial}{\partial t} \right) U = 0, \quad (6)$$

where U denotes the seismic wavefield and s is the slope, which can vary in both time and space coordinates. The time-space derivative of the plane wave equation is equivalent to the convolution operator $G(\theta)$ applied to the data (seismic wavefield)

$$G(\theta)U = 0. \quad (7)$$

The orientation θ in equation (7) is related to the slope s in equation (6). The convolution operator can be efficiently constructed using steerable filters. When the steerable filter orientation is perpendicular to the feature orientation in the image,

the output is zero (Freeman and Adelson, 1991). The local-slope (i.e., orientation) is determined efficiently at each data sample from its neighbors by spanning all possible orientations to find the orientation corresponding to the minimum amplitude of the steerable filter outputs (e.g., minimizing equation 7). The range of orientations corresponds to different apparent velocities of both the signal and noise. An instantaneous slowness (local-slope) plot is constructed. The table of instantaneous slowness (i.e., local-slope or orientation) constructed using steerable filters is modified to vary only laterally across the record as a function of offset by finding a single orientation that has maximum occurrences within each time-offset range

$$\hat{\theta}_n(x) = \arg \max_{\theta} P(\theta, x), \theta = 0, 1, \dots, 90^\circ, \quad (8)$$

where $\hat{\theta}_n(x)$ is the dominant local-slope as a function of offset (i.e., noise orientation), and $P(\theta, x)$ is the probability as a function of orientation and offset.

Signal and noise separation

The input data d consists of unknown signal d_s and noise d_n

$$d = d_s + d_n. \quad (9)$$

The application of the non-linear local median filter (Duncan and Beresford, 1995) predicts the data component (i.e., noise) that is aligned with the orientation $\hat{\theta}_n$ and attenuates all other components (i.e., signal) with different orientations

$$\begin{aligned} f(\hat{\theta}_n)d_s &= 0 \\ f(\hat{\theta}_n)d_n &= d_n, \end{aligned} \quad (10)$$

where $f(\hat{\theta}_n)$ is the filter operator steered toward the noise orientation, and d_s and d_n are the signal and noise components, respectively. The modified table of spatially varying slopes is used for steering the median filter toward the noise direction. For each temporal point within a window of receivers, we apply a $2M$ -point steered median filter to the data

$$d[m, n] = \text{median}\{f[i, j]\},$$

$$(i, j) \in \begin{aligned} & i - M \leq i \leq i + M \\ & j - M \cdot \tan(\hat{\theta}_n) \leq j \leq j + M \cdot \tan(\hat{\theta}_n) \end{aligned} \quad (11)$$

where $d[m, n]$ is the data point at the m trace and n time sample, i and j are the sample index in the spatial (x) and temporal (t) directions, respectively, and $\hat{\theta}_n$ is the orientation (i.e., slope) of the noise component to be removed. The center and median values of the time-space window should be very similar and represent the amplitude value of the estimated noise component when there is no reflection (signal) information ($f(\hat{\theta}_n)d_n = d_n$). However, if there are reflections, the value of the center sample will be replaced by the median value of it is neighboring points ($f(\hat{\theta}_n)d_s = 0$). Therefore, the application of this filter on the total data will predict only the noise component

$$\begin{aligned} f(\hat{\theta}_n)d &= f(\hat{\theta}_n)(d_s + d_n) \\ &= f(\hat{\theta}_n)d_n + f(\hat{\theta}_n)d_s \\ &= d_n. \end{aligned} \quad (12)$$

Hence, the signal component (d_s) is obtained by subtracting the predicted noise (d_n) from the input data (d)

$$\begin{aligned} d_s &= d - d_n \\ &= d - f(\hat{\theta}_n)d. \end{aligned} \quad (13)$$

Suppression of near-surface scattered body to surface waves

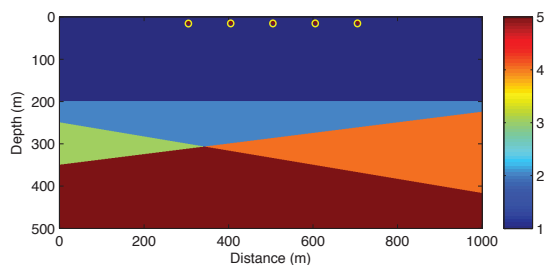


Figure 4: Synthetic earth model. Multiple dipping layers with five circular scatterers (red circles near the free surface) embedded in the shallow layer. Material properties are given in Table 1. The source is located at $(x,z)=(150\text{ m}, 0\text{ m})$, and receivers on the surface with 50 m near-offset and 5 m space intervals. The color scale (on the right) refers to layer numbers.

SYNTHETIC EXAMPLE

We illustrate, with a numerical example, the application of noise separation based on spatially varying slopes. To fully model elastic waves in the presence of heterogeneity, we utilize an accurate implementation of the standard staggered-grid (SSG) finite-difference scheme (Virieux, 1986; Levander, 1988; Zhang, 2010) that is fourth order accurate in space (including the free surface boundary) and second order accurate in time. We consider a two-dimensional earth model with multiple dipping layers and five scatterers embedded in the uppermost layer (Figure 4). The scatterers are located at 15 m depth below the free surface, and each has a 10 m diameter and an impedance contrast corresponding to 0.36. The material properties are given in Table 1. The domain has $N_x = 1001$ and $N_z = 501$ grid points with 1 m grid spacing (i.e., Δx and Δz), that is, 500 m depth (along the z -axis) and 1000 m distance (along the x -axis). The grid size is small enough to capture the shape of the scatterers. The time step is 0.2 ms. A vertical source is used with a Ricker wavelet and 30 Hz central frequency (~ 75 Hz maximum frequency). The source is located at $(x,z) = (150\text{ m}, 0\text{ m})$ and the receivers are located on the surface with 50 m near-offset and 5 m space intervals. We consider only the vertical component (v_z) of the particle velocity field. The scatterers are treated in the numerical scheme as a density and velocity perturbation. Calculated waveforms for the scattering model with and without the direct surface waves are shown in Figure 5. The direct and back-scattered surface waves are removed as they are much larger in amplitude than the scattered body-to-surface waves. This is achieved by computing the wavefield for a homogeneous full-space, with and without the near-surface scatterers, and then subtracting the direct surface waves from the incident and total wavefields, respectively, to isolate the scattered body waves. The effective medium properties of the heterogeneities are wavelength dependent.

All upcoming body wave reflections (e.g., primaries, multiples, and mode-conversions) scatter close to the free surface due to near-surface heterogeneities and, therefore, excite scattered surface waves. The scattered surface wave noise cov-

Material Index	α (m/s)	β (m/s)	ρ (kg/m ³)
1 - Dark blue	1800	1000	1750
2 - Blue	2200	1200	1900
3 - Green	2500	1300	2000
4 - Orange	2700	1400	2100
5 - Red	3000	1500	2250

Table 1: Material properties (P-wave velocity, S-wave velocity, and density) of the model shown in Figure 4.

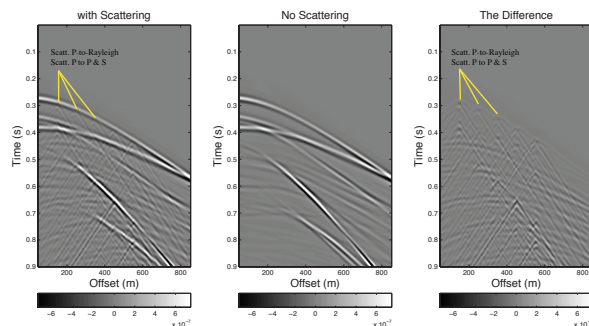


Figure 5: Finite-difference simulations (v_z) showing the scattering effects due to near-surface heterogeneities for the model in Figure 4: (left) total wavefield simulated using the model with scattering; (middle) incident wavefield simulated using the model without scattering; and (right) scattered wavefield.

ers the whole time-space domain with locally-linear features that propagate in both the positive and negative (i.e., forward and backward) directions. The scattered surface waves are more sensitive to the uppermost earth layer. Therefore, their slope can vary with offset due to lateral velocity variations (i.e., mostly shear-wave velocity) and surface topography. However, the surface waves exhibit constant local-slope (i.e., slowness) at each receiver location. Because the local-slope of the noise can only vary spatially with different receiver locations (or patch of receivers), only a small range of slopes is filtered at each offset unlike a global velocity filter. The process consists of four steps:

1. Dip decomposition: using a velocity filter (e.g., $f - k$ domain) to reduce the signal-noise interference such that the slope estimation yields a more reliable result.
2. Steerable filters: compute the directional derivatives (equation 7) of the dip-decomposed image for different supplementary orientations, and construct an instantaneous slowness table corresponding to the minimum amplitude of the steerable filter outputs.
3. Prediction: estimate the dominant local-slope of the noise component $\hat{\theta}_n(x)$ as a function of offset (or patch of offsets), as shown in Figure 6, by estimating the mode of the probability mass function of the instantaneous slowness values (equation 8).
4. Separation: apply spatially varying directional non-linear filter steered toward the noise directions (i.e., dominant local-slopes predicted in step 3) to predict the noise and then subtract it from the data (equations 11 to 13).

Suppression of near-surface scattered body to surface waves

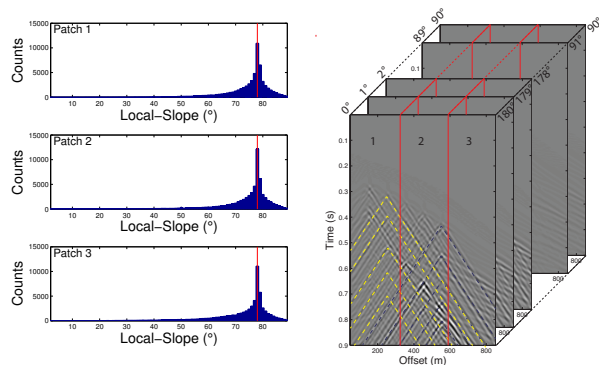


Figure 6: Histogram distributions of local-slopes calculated using steerable filters (left) for different receiver patches (right). The red lines in the histogram plots correspond to the true orientation of the forward and backward scattering.

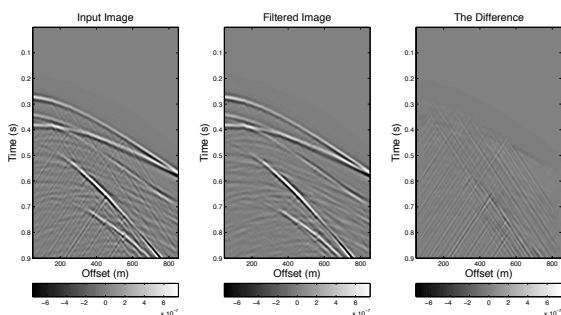


Figure 7: Application of the median filter: (left) input data, (middle) filtered data, and (right) the difference.

Histograms of local-slopes calculated using steerable filters for three patches of offsets from one shot gather are shown in Figure 6. The estimated dominant local-slopes match the true slopes of the noise components in all cases. The histograms look identical (because $f-k$ values are about the same). The offset patches allow for spatially varying slope estimation, which can be useful in the case of lateral shear wave velocity variations near the earth's surface. Each orientation represents applying the directional derivative at the supplementary angles (θ) and ($180^\circ - \theta$). Similarly, the recorded scattered surface waves propagating at the forward and backward directions have supplementary angles (i.e., slopes) at each offset location. The operator of the non-linear median filter steered toward the dominant supplementary slope directions returns the amplitude of the surface wave when there is no reflection interference, and it replaces the amplitude of the sample with its median of neighboring samples when reflections are present. The results of separating the signal and noise components are shown in Figure 7. The estimated signal is free of the scattered body-to-surface wave noise, and only very weak scattered P waves that have slopes similar to the reflected signal are passed by the filter. We compare the simulated data after applying our filtering approach and the conventional $f-k$ filter (Figure 8). The $f-k$ filter suffers from edge effects as well as smearing caused by leakage in the transform domain.

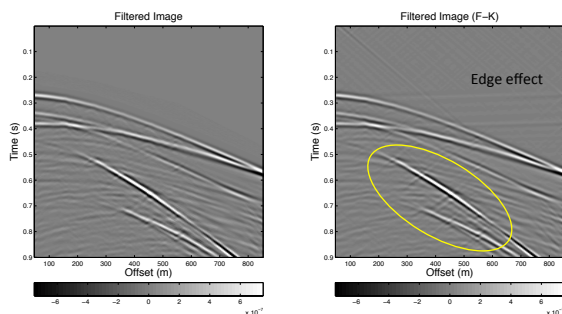


Figure 8: Comparison between (left) the directional filter, and (right) $f-k$ filter. Note the edge effects and smearing of reflected signal caused by the $f-k$ filter.

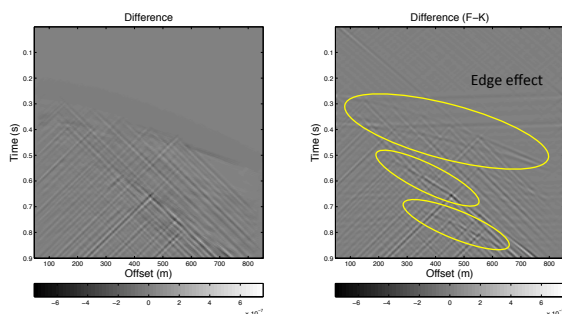


Figure 9: Difference between the input and filtered data in Figure 8: (left) directional filter and (right) $f-k$ filter. Note that the $f-k$ filter removed part of the reflected signal.

$f-k$ filtering also removed part of the signal, as shown in Figure 9, which directional filtering has preserved. The spatially varying slope filter has a narrow reject band in the $f-k$ domain that minimizes signal distortion.

DISCUSSION AND CONCLUSION

In this paper, we presented an approach to estimate dominant local-slopes in the data as a function of offset (or patch of offsets) using steerable filters and to separate the signal and noise components using a directional median filter. The slope estimation step using steerable filters requires only a linear combination of a set of basis filters at fixed orientation to synthesize an image filtered at an arbitrary orientation. This makes the process very efficient. The method can handle different slopes, locally-linear coherent noise that has small amplitude contrast and varying slope with offset. We successfully implemented this approach on synthetic data for the separation of scattered surface waves from reflected body-waves. The results show that this approach is superior to conventional $f-k$ techniques.

ACKNOWLEDGMENTS

We thank Saudi Aramco and ERL founding members for supporting this research.

Suppression of near-surface scattered body to surface waves

REFERENCES

- AlMuhaidib, A. M., and M. N. Toksöz, 2014, Numerical modeling of elastic wave scattering by near-surface heterogeneities: *Geophysics* (in press).
- Duncan, G., and G. Beresford, 1995, Median filter behaviour with seismic data: *Geophysical prospecting*, **43**, 329–345.
- Fomel, S., 2002, Applications of plane-wave destruction filters: *Geophysics*, **67**, 1946–1960.
- Freeman, W. T., and E. H. Adelson, 1991, The design and use of steerable filters: *IEEE Transactions on Pattern analysis and machine intelligence*, **13**, 891–906.
- Levander, A. R., 1988, Fourth-order finite-difference P-SV seismograms: *Geophysics*, **53**, 1425–1436.
- Simoncelli, E. P., and W. T. Freeman, 1995, The steerable pyramid: A flexible architecture for multi-scale derivative computation: *Image Processing, 1995. Proceedings., International Conference on*, IEEE, 444–447.
- Virieux, J., 1986, P-SV wave propagation in heterogeneous media: Velocity-stress finite-difference method: *Geophysics*, **51**, 889–901.
- Zhang, Y., 2010, Modeling of the effects of wave-induced fluid motion on seismic velocity and attenuation in porous rocks: PhD thesis, Massachusetts Institute of Technology.